HOKKAIDO UNIVERSITY

Title	Comparison of vegetation patch dynamics after the eruptions of the volcano Mount Usu, northern Japan, in 1977-1978 and 2000, detected by imagery chronosequence
Author(s)	Végh, Lea; Tsuyuzaki, Shiro
Citation	Ecological Research, 36(2), 329-339 https://doi.org/10.1111/1440-1703.12199
Issue Date	2021-03
Doc URL	https://hdl.handle.net/2115/84216
Rights	This is the peer reviewed version of the following article: Végh, L., Tsuyuzaki, S. Comparison of vegetation patch dynamics after the eruptions of the volcano Mount Usu, northern Japan, in 1977-1978 and 2000, detected by imagery chronosequence. Ecological Research. 2021; 36: 329-339, which has been published in final form at https://doi.org/10.1111/1440-1703.12199. This article may be used for non-commercial purposes in accordance with Wiley Terms and Conditions for Use of Self-Archived Versions.
Type	journal article
File Information	FinalVersion_Comparison of vegetation patch dynamics_Vegh.pdf

Hokkaido University Collection of Scholarly and Academic Papers : HUSCAP

This is the peer reviewed version of the following article:
[Végh, L, Tsuyuzaki, S. Comparison of vegetation patch dynamics after the eruptions of the volcano Mount Usu, northern Japan, in 1977–1978 and 2000, detected by imagery chronosequence. Ecological Research. 2021; 1– 11.],
which has been published in final form at [https://doi.org/10.1111/1440-1703.12199].
This article may be used for non-commercial purposes in accordance with Wiley Terms and Conditions for Use of Self-Archived Versions.

Comparison of vegetation patch dynamics after the eruptions of the volcano Mount Usu, northern Japan, in 1977-78 and 2000, detected by imagery chronosequence

Lea Végh[1] and Shiro Tsuyuzaki[1]
[1]Graduate School of Environmental Science, Hokkaido University, Japan

Correspondence
Lea Végh, Graduate School of Environmental Science, Hokkaido University, N10 W5, Sapporo, Japan, 060-0810
Email: vegh@eis.hokudai.ac.jp

Abstract
Vegetation patch dynamics were analysed to detect vegetation development patterns after eruptions on two sites (summit destroyed in 1977-78, and a foothill, Konpira destroyed in 2000) on the volcano Mount Usu, in northern Japan. Aerial photos and satellite images taken in 2000, 2006, and 2014 were used to develop an imagery chronosequence of vegetation patch dynamics. Vegetation patches were identified by the Normalized Difference Vegetation Index (NDVI) for satellite images, and by the Normalized Green-Red Difference Index (NGRDI) for aerial photos. We categorized the vegetation patch types based on whether the patches overlapped (touching) or not (isolated) with the future vegetation patches and whether their area increased (growing) or decreased (shrinking). Afterwards, patch dynamics were compared between the two sites through changes in patch types, dense vegetation, and patch growth with slope degree, elevation, and time. Isolated patches were established more at the summit and showed high mortality, while at Konpira most isolated patches survived until 2006 and merged into touching patches by 2014. Moreover, the vegetation density of patches was higher at Konpira than at the summit. Patch growth was associated with patch types at both sites. However, the time was more important for the patch dynamics at the summit, and the vegetation density affected the dynamics more at Konpira. Therefore, the two sites had different vegetation patch dynamics, which were related to the characteristics of topography and eruptions. In conclusion, the imagery chronosequence proposed in this study monitored patch dynamics well, and patches developed faster at Konpira.

Keywords: vegetation patch dynamics, revegetation, remote sensing, succession rate, volcanic eruption

1. Introduction

Succession is studied through the chronosequence approach, though caution should be taken with interpretation, because of the exclusion of stochastic and unpredictable processes, and the assumption of homogenous successional sere (Buma et al., 2019; Johnson & Miyanishi, 2008). Therefore, long-term monitoring of permanent plots is crucial to detect spatio-temporal vegetation changes to compensate the weakness of the chronosequence approach (Fischer et al., 2019). However, long-term field monitoring is constrained by time consumption and inaccessibility, particularly on volcanoes. In addition, vegetation patch dynamics should be investigated on a large scale, such as at landscape level, when large areas are disturbed (Prach & Walker, 2020).

Harsh environments formed by catastrophic disturbances restrict plant colonization and establishment (Chapin & Bliss, 1989). Vegetation patches, defined as a cluster of plants (Pickett & White, 1985), alleviate the harsh environments, particularly in the early stages of succession, although the role of vegetation patches in revegetation are unclear (Prach & Walker, 2020). The impact of vegetation patches on plants in and around the patches is positive (facilitation) or negative (inhibition), and is dependent on the size and growth rate of the patch-forming plants (Brooker et al., 2008). Therefore, clarifying vegetation patch dynamics is key to predicting the trajectory of succession.

Remote sensing is capable to investigate vegetation patch dynamics at landscape level (White et al., 2017). For example, time-series satellite images from the first 15 years after the 1980 catastrophic eruption on Mount St. Helens, USA, detected that disturbance intensity affects the pattern and pace of revegetation (Lawrence & Ripple, 2000). So far, remote analyses have mostly been conducted at pixel level (De Rose et al., 2011; De Schutter et al., 2015).

When such time-series analysis of remotely sensed data is applied to investigate vegetation patch dynamics, the dynamics may be clarified in more detail at landscape level. However, there are some obstacles when creating time-series analysis: high resolution images are often not available from the sensor for long periods and there are inaccuracies when overlaying images which hinder pixel level comparisons. To reduce these disadvantages, we investigated vegetation patch dynamics by images obtained from different platforms and focused on clusters of pixels. Here, we call this approach

imagery chronosequence. The combination of images from various sensors, i.e., aerial and satellite images, provides high resolution, long term coverage. Using clustered pixels reduces the inaccuracies of images and also improves the analysis of vegetation patches. A vegetation patch includes multiple plants, and changes in the size and vegetation density can be followed at cluster level but not at single pixel level.

Vegetation density within patches, which is often evaluated by vegetation indices (VIs), increases during the early to middle stages of succession, then decline again with aging, if the environments are unsuitable (Cipriotti & Aguiar, 2015). This indicates that vegetation density is diverse even for the same patch size and is related to vegetation patch dynamics. In addition, the numbers of newly established and persevering patches are affected by geological factors, represented by elevation and slope degree (Tsuyuzaki, 1995; Walker & del Moral, 2003). Therefore, vegetation patch dynamics were analysed by variations in the number, size and vegetation density of patches in relation to elevation and slope degree on each patch.

The first aim of this study was to examine the applicability of imagery chronosequence using different sources of images; and second one was to evaluate vegetation patch dynamics by the growth and vegetation density of the patches with two abiotic factors, elevation and slope degree, both of which were plausible to determine vegetation patch dynamics. To confirm these, two eruption sites on Mount Usu, northern Japan, were used.

2. Methods

2.1 Study area

Mount Usu is a basalt-andesite stratovolcano in Hokkaido Island, northern Japan (42°32’N, 140°50’E, 733 m elevation) with frequent eruptions (Katsui et al., 1981). The mountain belongs to the temperate zone, with an average annual precipitation of 891 mm and annual mean temperature of 8°C during 1976-2018 (Date Meteorological Station at 5 km from Usu; JMA 2019). The climax vegetation is a deciduous oak or mixed broad-leaved forests in the lowlands of this region, including Mount Usu (Okitsu, 2003).

The last two eruptions occurred at two different sites, the summit in 1977-78 and a foothill called Konpira in 2000. The major volcanic ejecta were volcanic ash and pumice at the two sites (Obase et al., 2008; Tsuyuzaki, 1989). The eruptions denuded both areas, although the eruption scale was smaller at Konpira (Table 1). The summit is 340 m higher in elevation than Konpira. The summit was covered with seeded pastures and broad-leaved forests dominated by pioneer trees prior to the eruptions (Tsuyuzaki, 1987), and natural revegetation occured mostly by vegetative reproduction of large perennial forbs soon after the eruptions (Tsuyuzaki, 1989) and then replaced by broadleaved forests. Konpira was covered mostly with broad-leaved forests and plantations of needle-leaved trees before the eruptions (Obase et al., 2008), and the revegetation has been promoted mostly by pioneer forbs and trees until now.

2.2 Analysis of aerial and satellite images

Image analysis was carried out by ArcGIS (ver. 10.2, ESRI) in WGS 1984 UTM zone 54N projection system. The satellite images were acquired on 8 September 2006 (QuickBird, resolution 2.4 m) and 1 August 2014 (Ikonos, resolution 3.2 m), while the aerial photographs were taken on 14 August 2000 (obtained from the Geospatial Information Authority of Japan). The satellite images were ortho-rectified by the Digital Elevation Model provided by the Geospatial Information Authority of Japan (accuracy within 0.7m, resolution 6.2 m). After the ortho-rectification a small misalignment remained between the images, and was manually corrected by georeferencing the Ikonos image to the Quickbird image using zero order polynomial transformation (i.e. shifting the image). Afterwards, the digital numbers of the satellite images were converted to top of atmospheric reflectance (Krause, 2003; Taylor, 2009). Because the aerial photographs lacked spatial reference, the photographs were georeferenced to the Quickbird image using geographical features (spline transformation). Finally, the Quickbird and aerial images were resampled to 3.2 m pixel resolution.

The blue, green, red, and near-infrared (NIR) bands of the satellite images were used for calculating the Normalized Difference Vegetation Index (NDVI) = (NIR - red)/(NIR + red) (Rouse et al., 1974), and the blue, green, and red bands of the aerial images were used to calculate the Normalized Green-Red Difference Index (NGRDI) =

(green - red)/(green + red) (Gitelson et al., 2002), depending on the wavelength range of the sensors; NDVI was used for satellite images and NGRDI for aerial photo images. We chose these indices because NDVI was shown to classify vegetation cover well fifteen years after the eruptions on Mount St. Helens (Lawrence & Ripple, 1998), and because NGRDI is a good alternative to NDVI if NIR is not present (Rasmussen et al., 2016). However, to test the similarity of NDVI and NGRDI, both VIs were calculated from satellite images, and the Pearson's correlation coefficient of pixel values was examined.

Supervised maximum likelihood classification (37 training areas) on the VI images categorized land cover into no vegetation cover (bare ground and water surface), sparse, and dense vegetation cover. Sparse and dense vegetation cover was separated roughly by VIs, i.e. dense vegetation cover showed higher VI than sparse cover (Supporting information, Table S1). Additionally, the field observations in 2014-15 confirmed that the sparse and dense vegetation cover consisted largely of short (mostly herbs and shrubs) and tall plants (mostly trees), respectively. However, further improvement was required as shown below. To eliminate misclassified pixels, the classified images were generalised by dissolving areas less than 3 pixels in size. Thus, the completed maps detected the locations and sizes of patches larger than 20 m^2 that was covered by two pixels or more. The accuracy of patch classification was assessed by Kappa coefficients on randomly-selected points on the maps. In total, 100 and 200 points were selected at Konpira and the summit, respectively, in each image acquisition year, 2000, 2006, and 2014. The Kappa coefficients were obtained by the confusion matrices of the relationships between classification by VIs and visual validation (Cohen, 1960). Areas altered by erosion control works by the Forest Agency of Japan, such as artificial seeding, plantation and embankment, were removed from the completed maps.

2.3 Measurements of patch characteristics

The study was divided into two observation periods: the first observation period was from 2000 to 2006 and the second was from 2006 to 2014. The vegetation patches were classified into two types, "touching" and "isolated" to investigate different dynamics between persisting and transient patches (Figure 1). Touching patches were defined as

patches present throughout the observation periods, whereas isolated patches were present only at the first or final census during each period. When patches merged or split, the patches were handled as a patch group (touching), and the patch size was calculated as the sum of the area of the individual patches.

Assuming patch shape to be circular, the annual growth was expressed by the change of radius: (radius of the final observation year – radius of the first year)/(years between the two observations). The radius was zero in the first or final observation year for isolated patches. Positive and negative annual growths indicated that the patches were "shrinking" and "growing", respectively. Therefore, there were four categories of patch growth types: isolated and touching patches by shrinking and growing patches. The patch mortality during each period was calculated by (the number of isolated patches disappeared by the end of period) / (the total number of patches). When analysing annual growth, patches whose growth was artificially restricted to zero (8 patches at the summit and 20 patches at Konpira) were excluded from the analyses.

To consider the effect of initial patch size on patch dynamics, proportional change of area (rate of change) for touching patches was calculated as the geometric mean of the area at the start and end of the period. The vegetation density of the patches (%) was calculated as: (area of sparse vegetation cover) / (area of total cover) by 100. For touching patches, the vegetation density was averaged between the first and final year of the period. Slope degree and elevation on each patch was calculated from the digital elevation model using weighted mean within the patch, and was averaged for touching patches between the first and final year of the observation periods.

2.4 Statistical analyses

Generalized linear models (GLMs) were used to investigate the changes in vegetation patches, because of the non-normal distribution (Shapiro-Wilk normality test, $P \leq 0.01$). The numbers of growing and shrinking patches were compared by GLMs with binominal distribution and logit link (Bates et al., 2015). The explanatory variables were eruption sites, patch types, and observation periods. Since the interactions between the explanatory variables were not significant, the interactions were not included in the analyses. Differences in slope degree, elevation, patch size and vegetation density on

touching and isolated patches were compared between the two sites by Wilcoxon signed rank test and Kruskal-Wallis test, as these tests work without specifying the distribution. The ratio of newly vegetated areas to the total eruption areas showed normal distribution (Shapiro-Wilk normality test, $P = 0.45$) and was analysed with linear model (LM) using eruptions sites as explanatory variables.

Because patches often increase their vegetation densities without changes in their sizes, vegetation density and patch growth were analysed separately. For investigating the factors affecting vegetation density of the patches, GLMs were used with logistic binomial regression on the respective eruption sites. When analysing the two sites together, the site was coded as a categorical variable. The explanatory variables were observation period, patch type, slope degree, and elevation. Fittest model to explain vegetation density of the patches was obtained by backward procedure. The initial model contained all the variables. Then, less significant variables were removed until the model became stable, indicated by the F-values of analysis of variance. Significance level was adjusted to $P < 0.01$ to reduce Type I error.

The annual growth of patches was transformed to absolute values and analysed by GLMs with Gamma distribution and log link. Including vegetation density as explanatory variable distorted the analysis at the summit, because 96% of the patches had sparse vegetation. Therefore, the explanatory variables at the summit were observation period, patch type, slope, and elevation. At Konpira, vegetation density was included among the variables. The interactions between the explanatory variables were also examined. The rate of change of touching patches was examined using the same variables and GLMs. The spatial-autocorrelation of patch growth on the final model was examined by Moran's I with the coordinates of the patches. Statistical analyses were carried out using R software (ver. 3.5.1, R Core Team, 2018).

3. Results

3.1 The accuracy of vegetation indices and classification

The Pearson's correlation coefficients (r) between NDVI and NGRDI of the same satellite images were higher than 0.85 in both 2006 and 2014 at the summit ($P < 0.001$,

Table 2). Open water surfaces at Konpira were evaluated differently by the VIs, but removed from the analysis, *r* was 0.60 in 2006 and 0.90 in 2014, respectively ($P < 0.001$, Supporting information, Figure S1). Therefore, the vegetation patches identified by NDVI and NGRDI were comparable.

The NGRDI-based patch distribution map of 2000 and the NDVI-based maps of 2006 and 2014 had high classification accuracy (Table 3). The Kappa coefficients were 0.95, 0.98 and 0.99 for the 2000, 2006 and 2014 images, respectively. In addition, field observations of a subset of the sites (46 points at the summit and 17 points at Konpira) supported that misclassification was low. Hence, the location and vegetation density of patches were detected with high accuracy.

3.2 Comparison of eruption sites

The study area at the summit was 291 ha while that at Konpira encompassed 38 ha (Table 1). The slope degree of the sites averaged 25° with a maximum of 85° at the summit and 26° with a maximum of 88° at Konpira. Therefore, the slope degrees did not differ greatly between the two sites.

The numbers of growing and shrinking patches differed between the sites, patch types and observation periods (Table 4). The maximum patch densities at the summit were 2.32/ha and 1.61/ha during 2000-2006 and 2006-2014, respectively. The densities at Konpira were 2.96/ha and 1.04/ha. The ratio of shrinking patches to the total was higher at the summit than at Konpira (GLM, $P < 0.001$, $z = 5.9$), but increased at both sites during the second period ($P < 0.001$, $z = 5.7$). The increased ratio of shrinking patches was due to the low number of growing isolated patches in the second period. Touching patches had a higher ratio of growing patches than isolated patches during the surveyed periods ($P = 0.01$, $z = -2.5$). Although the isolated patches outnumbered touching patches in both periods, the ratios of isolated patches decreased from the first to the second periods. The increased ratio of touching patches with the decrease in patch density at both sites indicated that a number of isolated patches in the first period merged by the end of second period, especially at Konpira.

Slope degrees where the patches established were not different between the two sites (Table 4), but the elevation of patches was higher at the summit than at Konpira.

Isolated patches established at lower elevation than the touching patches at the summit (Wilcoxon rank sum test, $P < 0.001$). The sizes of touching patches were comparable at the two sites, and were larger than isolated patches. In contrast, the isolated patches were smaller at the summit than at Konpira, although the statistical significance was low ($P = 0.02$). The touching patches developed more dense vegetation than the isolated patches at the two sites. However, the vegetation density of isolated patches at Konpira did not differ from that of the touching patches at the summit. While the difference between the mean of sparse cover ratios of isolated and touching patches was 7% at the summit, the mean was approximately 50% at Konpira.

Patch establishment had already proceeded on the edges of the crater at the summit in 2000 after the 1977-78 eruptions (Figure 2a). Afterwards, the patch establishment progressed to the centre of the crater, but the ratio of newly vegetated area was only 17% in the first and 3% in the second period (Figure 2b-d). Likewise, the patch establishment started on the edges of the crater at Konpira (Figure 2e-f). Since the eruption at Konpira occurred in 2000, the initial stage of patch establishment was clearly detected from 2000 to 2014 (Figure 2e-h), and more areas became newly vegetated in the first and second periods with 40% and 37%, respectively, than at the summit (LM, $P = 0.05$, $t = -4.1$). At Konpira, 83% of the area was covered with vegetation by 2014; while vegetation covered 57% of the summit leaving the central area largely bare. In addition, the patch mortality at the summit was over 30% in both periods, while the mortality at Konpira was low, under 10%, during these periods. These results indicated that most isolated patches in the first period persisted and became touching patches in the second period at Konpira.

3.3 Effects of topography on patch vegetation density

GLM with logistic regression showed that at the summit, both elevation and slope degree negatively affected the vegetation density when the opposing factor was excluded ($P < 0.05$). As slope degree did not differ between isolated and touching patches (Table 4), the slope degree was retained in the model and elevation was discarded. The touching patches were significantly denser than isolated patches ($P < 0.001$, $z = -4.8$, $df = 955$). Both isolated and touching patches became sparsely

vegetated as the slope degree increased at the summit, although the significance was low ($P = 0.03$, $z = 2.2$, $df = 955$, Figure 3a). The negative effect of slope was weak in the isolated patches, as their vegetation cover was sparse even on gentle slopes. These results indicated that steep slopes did not decrease patch establishment, but negatively affected the development of dense vegetation cover.

At Konpira, only the patch type influenced vegetation density. The touching patches had denser vegetation than the isolated patches ($P < 0.001$, $z = -4.7$, Figure 3b), but period, elevation, slope degree, and patch size did not affect the vegetation density of the patches.

3.4 Annual growth of patches

Slope degree, patch size, and elevation did not affect the annual growth at the summit, but the patch type and observation period did (Table 5). The touching patches displayed faster positive or negative growth than the isolated patches ($P < 0.001$, $t = 4.2$, $df = 946$), while all patches showed slower size change during the second period ($P < 0.001$, $t = -4.2$). The decrease of annual growth was more pronounced for the touching patches than for the isolated patches in the second period ($P < 0.001$, $t = -8.0$).

The elevation and patch size did not influence annual growth at Konpira, but in contrast to the summit, observation period and slope degree also did not affect growth. The annual growth of patches was determined by the patch type and vegetation density; the touching patches changed their area faster than the isolated patches (Table 5, $P = 0.006$, $t = 2.8$, $df = 100$), and the dense patches, not depending on their type, grew faster than the sparse patches ($P < 0.001$, $t = -3.9$).

The annual growth was slower at the summit than at Konpira (GLM, $P < 0.001$, $t = -8.2$, $df = 1048$). The difference was mainly due to the large variation of patch growth at Konpira (Figure 4), where a few touching patches grew fast due to multiple patches merging together. The residuals of the patch growth models did not show spatial auto-correlation at the summit and at Konpira ($I = –0.003$, $P = 0.68$ and $I = 0.003$, $P = 0.41$, respectively).

Of the touching patches, the growing patches showed larger rate of change than the shrinking patches at the summit (GLM, $P < 0.001$, $t = 11.4$, $df = 179$). All patches

decreased their rate of change during the second period (P = 0.003, t = -3.0). At Konpira, both slope degree and elevation had significant effects on proportional change. Steeper slopes showed an accelerated rate of change (P = 0.003, t = 9.4, df = 3), while higher elevation slowed the rate of change (P < 0.001, t = -26.7). Likewise to the summit, the growing patches increased their size quickly (P < 0.001, t = 18.5), and the rate of change of patches slowed during the second period (P < 0.001, t = -26.0).

4. Discussion

4.1 Applicability of imagery chronosequence

The imagery chronosequence used in this study was accurate based on the high Kappa coefficients. This technique can be applied to various time-series analysis, although further improvement is desirable to objectively compare with field surveys, e.g., calibration with ground VI measurements. So far, pixel-based analysis has been popular for analysing vegetation (De Rose et al., 2011; Lawrence & Ripple, 2000), partly due to the widespread availability of course resolution imagery. However, vegetation patches cannot be extracted from course resolution images. Since revegetation is often promoted by vegetation patches after large disturbances (Prach & Walker, 2020), investigating vegetation patch dynamics on a large scale is important. The obstacle to examining patch dynamics is that good quality images captured over longer time periods are difficult to obtain (Loarie et al., 2008). The imagery chronosequence introduced here removed this obstacle and succeeded in detecting vegetation patches.

However, this approach is limited if high resolution observations are required. Because the focus is on clusters of pixels, the resolution of the analysis decreases. Investing in more image pre-processing steps and validation efforts will resolve this issue.

4.2 The effects of environments on vegetation patch dynamics

During the 15 years from 2000 to 2014, vegetation cover increased both at the summit and Konpira, progressing from the edges towards the centre of the craters. Both sites were surrounded by un-damaged forests, and the vegetation recovery started from these

refugia, a pattern also observed on Mount St. Helens (Lawrence & Ripple, 2000). However, isolated patches farther from the edge did not persist at the summit, so the central area still retained bare lands, whereas isolated patches persisted at Konpira and the plant cover extended.

This suggested that the proximity of plant sources induced fast immigration of plants in the early successional stages (Fuller & del Moral, 2003; Makoto & Wilson, 2016) and large disturbance scale slowed revegetation. Moreover, annual growth of the patches was slower and vegetation density of the patches was lower at the summit than at Konpira. Vegetation patches provide stable environments, protection from erosion and strong wind at high elevation (Marler & del Moral 2011; del Moral et al. 2010), although vegetation cover increases slowly with increasing elevation on Mount St. Helens (del Moral, 2007). These implied that the patches at the summit experienced more stress and grew more slowly.

The elevation difference was approximately 340 m between the two sites. Because the elevation differed greatly between the summit and Konpira, the elevation and its related factors should be more severe at the summit. Small elevational differences were related to the vegetation development patterns at the summit of Mount Usu (Tsuyuzaki, 2019), and high elevation slowed down succession on Mount Ontake, central Japan, because of the short growing season and low species diversity (Nakashizuka, Iida, Suzuki, & Tanimoto, 1993). Other factors, such as soil properties, species compositions and stochastic events also affect patch dynamics as well (del Moral et al. 2010; Wilmshurst & McGlone 1996; Zobel & Antos 2017). However, soil properties did not differ greatly between the two sites, and the species composition was comparable (Otaki, Takeuchi, & Tsuyuzaki, 2016; Tsuyuzaki, 2019). Therefore, the stresses caused by the elevation and its related environmental factors seemed to determine slow patch dynamics at the summit.

The vegetation density of patches was reduced on steep slopes at the summit. However, steep slopes sometimes provide suitable environments for revegetation on Mount St. Helens in USA and Mt. Pinatubo in Philippines, because the ground surfaces at steep slopes become stable soon after the eruptions due to soil erosion (De Rose et al., 2011; del Moral et al., 1995). In comparison, the ground surface instability persists for many years on Mount Usu due to the properties of the volcanic ejecta (Tsuyuzaki, 2009).

At Konpira, the slope degree did not affect the vegetation density of the patches, and all patches became densely vegetated as time passed. The responses of plants to slope degrees, which were different between the two sites, suggested that the slope degree hid the prime factors, such as ground surface stability.

4.3 Vegetation patch growth

The touching patches grew faster than the isolated patches, especially at Konpira. The fast growth of touching patches in the early stages is explained partly by vegetative reproduction, because the common species were derived from vegetative reproduction soon after the eruptions at the two sites on Mount Usu (Obase et al., 2008; Tsuyuzaki, 1989). Likewise on Mount St. Helens, vegetative reproduction quickly increases the cover when tephra is thin or removed (del Moral & Eckert 2005; Wilmshurst & McGlone 1996).

Between the two periods, the touching patches growth decreased faster than the isolated patches at the summit. Vegetation recovery rate decreases with the number of years increasing after eruptions, e.g. on Mount St. Helens (del Moral & Magnússon 2014), due often to an increase in inter- and intra-specific competition within patches (Endo et al., 2008). However, the vegetation patches act as seed traps and facilitate the seedling establishment (Tirado et al., 2005). Therefore, patches act as facilitators, even though competition is present (Cipriotti & Aguiar, 2015). The denser vegetation of touching patches suggested that the facilitation promoted increased density of plants instead of increased growth (Berdugo et al., 2019).

The patch dynamics at Konpira resulted in faster revegetation, by developing touching patches with low mortality. The isolation of vegetation patches delays succession on Mount St. Helens and Iceland's Surtsey (del Moral & Magnússon 2014), and the proximity of plant sources and patch connectivity had positive effects on the patch growth and vegetation density at Konpira. As patches at Konpira persisted more, the number of years that passed following the eruptions was less influential on patch development.

5. Conclusion

The imagery chronosequence presented here clarified the vegetation patch dynamics. These findings have never been obtained on a large scale by remotely sensed data. The revegetation was slower at the summit, likely due to the large distance to seed sources that induced slow patch growth and low patch survival. The touching patches developed denser vegetation than the isolated patches at the two sites, and the vegetation density of the patches positively correlated with the patch growth. Steep slopes showed more sparsely-vegetated patches at the summit, and showed less effect on the patches at Konpira. The imagery chronosequence can also detect stochastic events, which affect long-term vegetation patch dynamics at landscape level (del Moral et al., 2010; Wilmshurst & McGlone, 1996; Zobel & Antos, 2017). In conclusion, the imagery chronosequence is applicable to clarify revegetation investigated by vegetation patch dynamics, and further improvements can develop its potential.

Acknowledgements

The authors express their gratitude to the Japanese Ministry of Education, Culture, Sports, Science and Technology for supporting the study. We also thank Assistant Professor Kubo Takuya for his advice in statistical modelling and Dale Whitfield for proofreading the manuscript. A previous version of the manuscript was improved by the comments of two anonymous reviewers. The study was partly funded by the Japan Society for the Promotion of Science and Japan Aerospace Exploration Agency. The authors declare that they have no conflict of interest.

References

Bates, D., Mächler, M., Bolker, B., & Walker, S. (2015). Fitting Linear Mixed-Effects Models Using lme4. *Journal of Statistical Software, Articles*, *67*(1), 1–48. https://doi.org/10.18637/jss.v067.i01

Berdugo, M., Soliveres, S., Kéfi, S., & Maestre, F. T. (2019). The interplay between facilitation and habitat type drives spatial vegetation patterns in global drylands. *Ecography*, *42*(4), 755–767. https://doi.org/10.1111/ecog.03795

Brooker, R. W., Maestre, F. T., Callaway, R. M., Lortie, C. L., Cavieres, L. A., Kunstler, G., Liancourt, P., Tielbörger, K., Travis, J. M. J., Anthelme, F., Armas, C., Coll, L., Corcket, E., Delzon, S., Forey, E., Kikvidze, Z., Olofsson, J., Pugnaire, F., Quiroz, C. L., … Michalet, R. (2008). Facilitation in plant communities: The past, the present, and the future. *Journal of Ecology*, *96*(1), 18–34. https://doi.org/10.1111/j.1365-2745.2007.01295.x

Buma, B., Bisbing, S. M., Wiles, G., & Bidlack, A. L. (2019). 100 yr of primary succession highlights stochasticity and competition driving community establishment and stability. *Ecology*, *100*(12), e02885. https://doi.org/10.1002/ecy.2885

Chapin, D. M., & Bliss, L. C. (1989). Seedling Growth, Physiology, and Survivorship in a Subalpine, Volcanic Environment. *Ecology*, *70*(5), 1325–1334. JSTOR. https://doi.org/10.2307/1938192

Cipriotti, P. A., & Aguiar, M. R. (2015). Is the balance between competition and facilitation a driver of the patch dynamics in arid vegetation mosaics? *Oikos*, *124*(2), 139–149. https://doi.org/10.1111/oik.01758

Cohen, J. (1960). A Coefficient of Agreement for Nominal Scales. *Education and Psychological Measurement*, *20*(1), 37–46.

De Rose, R. C., Oguchi, T., Morishima, W., & Collado, M. (2011). Land cover change on Mt. Pinatubo, the Philippines, monitored using ASTER VNIR. *International Journal of Remote Sensing*, *32*(24), 9279–9305. https://doi.org/10.1080/01431161.2011.554452

De Schutter, A., Kervyn, M., Canters, F., Bosshard-Stadlin, S. A., Songo, M. A. M., & Mattsson, H. B. (2015). Ash fall impact on vegetation: A remote sensing approach of the Oldoinyo Lengai 2007–08 eruption. *Journal of Applied Volcanology*, *4*(1), 15. https://doi.org/10.1186/s13617-015-0032-z

del Moral, R. (2007). Limits to convergence of vegetation during early primary succession. *Journal of Vegetation Science*, *18*(4), 479–488. https://doi.org/10.1111/j.1654-1103.2007.tb02562.x

del Moral, R., & Eckert, A. J. (2005). Colonization of volcanic deserts from productive patches. *American Journal of Botany*, *92*(1), 27–36. https://doi.org/10.3732/ajb.92.1.27

del Moral, R., & Magnússon, B. (2014). Surtsey and Mount St. Helens: A comparison of early succession rates. *Biogeosciences*, *11*(7), 2099–2111. https://doi.org/10.5194/bg-11-2099-2014

del Moral, R., Saura, J. M., & Emenegger, J. N. (2010). Primary succession trajectories on a barren plain, Mount St. Helens, Washington: Primary succession trajectories. *Journal of Vegetation Science*, *21*(5), 857–867. https://doi.org/10.1111/j.1654-1103.2010.01189.x

del Moral, R., Titus, J. H., & Cook, A. M. (1995). Early primary succession on Mount St. Helens, Washington, USA. *Journal of Vegetation Science*, *6*, 107–120. https://doi.org/10.2307/3236262

Endo, M., Yamamura, Y., Tanaka, A., Nakano, T., & Yasuda, T. (2008). Nurse-Plant Effects of a Dwarf Shrub on the Establishment of Tree Seedlings in a Volcanic Desert on Mt. Fuji, Central Japan. *Arctic, Antarctic, and Alpine Research*, *40*(2), 335–342. https://doi.org/10.1657/1523-0430(07-013)[ENDO]2.0.CO;2

Fischer, D. G., Antos, J. A., Biswas, A., & Zobel, D. B. (2019). Understorey succession after burial by tephra from Mount St. Helens. *Journal of Ecology*, *107*(2), 531–544. https://doi.org/10.1111/1365-2745.13052

Fuller, R. N., & del Moral, R. (2003). The role of refugia and dispersal in primary succession on Mount St. Helens, Washington. *Journal of Vegetation Science*, *14*(5), 637–644. https://doi.org/10.1111/j.1654-1103.2003.tb02195.x

Gitelson, A. A., Kaufman, Y. J., Stark, R., & Rundquist, D. (2002). Novel algorithms for remote estimation of vegetation fraction. *Remote Sensing of Environment*, *80*(1), 76–87. https://doi.org/10.1016/S0034-4257(01)00289-9

JMA. (2019). *Date Meteorological Station*. Japan Meteorological Agency. https://www.data.jma.go.jp/obd/stats/etrn/view/annually_a.php?prec_no=21&block_no=0132&year=&month=&day=&view=

Johnson, E. A., & Miyanishi, K. (2008). Testing the assumptions of chronosequences in succession. *Ecology Letters*, *11*(5), 419–431. https://doi.org/10.1111/j.1461-0248.2008.01173.x

Katsui, Y., Yokoyama, I., & Murozumi, M. (1981). Usu volcano. In *Field excursion guide to Usu and Tarumai volcanoes and Noboribetsu spa*. Volcanological Society of Japan.

Krause, K. (2003). *Radiance Conversion of QuickBird Data*. DigitalGlobe.

Lawrence, R. L., & Ripple, W. J. (1998). Comparisons among Vegetation Indices and Bandwise Regression in a Highly Disturbed, Heterogeneous Landscape: Mount St. Helens, Washington. *Remote Sensing of Environment*, *64*(1), 91–102.

Lawrence, R. L., & Ripple, W. J. (2000). Fifteen years of revegetation of Mount St. Helens: A landscape-scale analysis. *Ecology*, *81*(10), 2742–2752. https://doi.org/10.1890/0012-9658(2000)081[2742:FYOROM]2.0.CO;2

Loarie, S., Joppa, L., & Pimm, S. (2008). Satellites miss environmental priorities. *Trends in Ecology & Evolution*, *22*, 630–632. https://doi.org/10.1016/j.tree.2007.08.018

Makoto, K., & Wilson, S. D. (2016). New Multicentury Evidence for Dispersal Limitation during Primary Succession. *The American Naturalist*, *187*(6), 804–811. https://doi.org/10.1086/686199

Marler, T. E., & del Moral, R. (2011). Primary succession along an elevation gradient 15 years after the eruption of Mount Pinatubo, Luzon, Philippines. *Pacific Science*, *65*(2), 157–173. https://doi.org/10.2984/65.2.157

Nakashizuka, T., Iida, S., Suzuki, W., & Tanimoto, T. (1993). Seed dispersal and vegetation development on a debris avalanche on the Ontake volcano, Central Japan. *Journal of Vegetation Science*, *4*(4), 537–542. https://doi.org/10.2307/3236081

Obase, K., Tamai, Y., Yajima, T., & Miyamoto, T. (2008). Mycorrhizal colonization status of plant species established in an exposed area following the 2000 eruption of Mt. Usu, Hokkaido, Japan. *Landscape and Ecological Engineering*, *4*(1), 57–61. https://doi.org/10.1007/s11355-008-0035-6

Okitsu, S. (2003). Forest Vegetation of Northern Japan and the Southern Kurils. In J. Kolbek, M. Šrůtek, & E. O. Box (Eds.), *Forest Vegetation of Northeast Asia* (pp. 231–261). Springer Netherlands. https://doi.org/10.1007/978-94-017-0143-3_7

Otaki, M., Takeuchi, F., & Tsuyuzaki, S. (2016). Changes in microbial community composition in the leaf litter of successional communities after volcanic eruptions of Mount Usu, northern Japan. *Journal of Mountain Science*, *13*(9), 1652–1662. https://doi.org/10.1007/s11629-016-3835-4

Pickett, S. T. A., & White, P. S. (1985). *The Ecology of natural disturbance and patch dynamics*. Academic Press. https://opac.lib.hokudai.ac.jp/opac/opac_link/bibid/2000019932

Prach, K., & Walker, L. R. (2020). Terrestrial Biomes. In *Comparative Plant Succession among Terrestrial Biomes of the World* (Ecology, Biodiversity and Conversation, pp. 20-50). Cambridge University Press.

R Core Team. (2018). *R: A language and environment for statistical computing* (3.5.1) [Computer software]. R Foundation for Statistical Computing. https://www.R-project.org/

Rasmussen, J., Ntakos, G., Nielsen, J., Svensgaard, J., Poulsen, R. N., & Christensen, S. (2016). Are vegetation indices derived from consumer-grade cameras mounted on UAVs sufficiently reliable for assessing experimental plots? *European Journal of Agronomy*, *74*, 75–92. https://doi.org/10.1016/j.eja.2015.11.026

Rouse, J. W., Haas, R. H., Schell, J. A., & Deering, D. W. (1974). Monitoring Vegetation Systems in the Great Plains with ERTS. *Proceedings of Third Earth Resources Technology Satellite-1 Symposium*, *1*, 48–62.

Taylor, M. (2009). *IKONOS Planetary Reflectance and Mean Solar Exoatmospheric Irradiance*. 3.

Tirado, R., Pugnaire, F. I., & Eriksson, O. (2005). Community Structure and Positive Interactions in Constraining Environments. *Oikos*, *111*(3), 437–444. JSTOR.

Tsuyuzaki, S. (1987). Origin of plants recovering on the volcano Usu, northern Japan, since the eruptions of 1977 and 1978. *Vegetatio*, *73*(1), 53–58.

Tsuyuzaki, S. (1989). Analysis of revegetation dynamics on the volcano Usu, northern Japan, deforested by 1977-78 eruptions. *American Journal of Botany*, *76*(10), 1468–1477. https://doi.org/10.1002/j.1537-2197.1989.tb15128.x

Tsuyuzaki, S. (1995). Vegetation recovery patterns in early volcanic succession. *Journal of Plant Research*, *108*(2), 241–248.

Tsuyuzaki, S. (2009). Causes of plant community divergence in the early stages of volcanic succession. *Journal of Vegetation Science*, *20*(5), 959–969.

Tsuyuzaki, S. (2019). Vegetation changes from 1984 to 2008 on Mount Usu, northern Japan, after the 1977–1978 eruptions. *Ecological Research*. https://doi.org/10.1111/1440-1703.12045

Walker, L. R., & del Moral, R. (2003). *Primary succession and ecosystem rehabilitation*. Cambridge University Press.

White, M. A., Cornett, M. W., & Wolter, P. T. (2017). Two scales are better than one: Monitoring multiple-use northern temperate forests. *Forest Ecology and Management*, *384*, 44–53. https://doi.org/10.1016/j.foreco.2016.10.032

Wilmshurst, J. M., & McGlone, M. S. (1996). Forest disturbance in the central North Island, New Zealand, following the 1850 BP Taupo eruption. *The Holocene*, *6*(4), 399–411. https://doi.org/10.1177/095968369600600402

Zobel, D. B., & Antos, J. A. (2017). Community reorganization in forest understories buried by volcanic tephra. *Ecosphere*, *8*(12), e02045. https://doi.org/10.1002/ecs2.2045

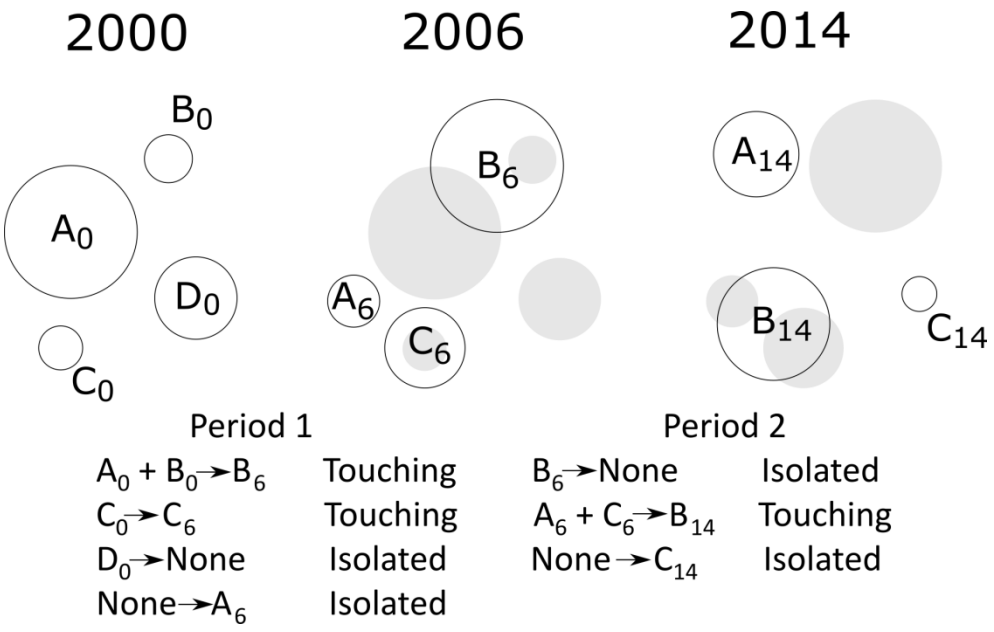

Figure 1. Patch classification based on persistency of the patches. Empty circles show patches present in the given year, while filled circles show the location of patches from the previous observation year (not present anymore). The respective patches are marked alphabetically with the subscript showing the year in which the patch is observed. Period 1 and 2 refers to 2000–2006 and to 2006–2014, respectively. As an example, patch B_6 is identified as touching patch during the first period, developing from the patch group A_0 and B_0. However, in the second period B_6 is identified as an isolated patch.

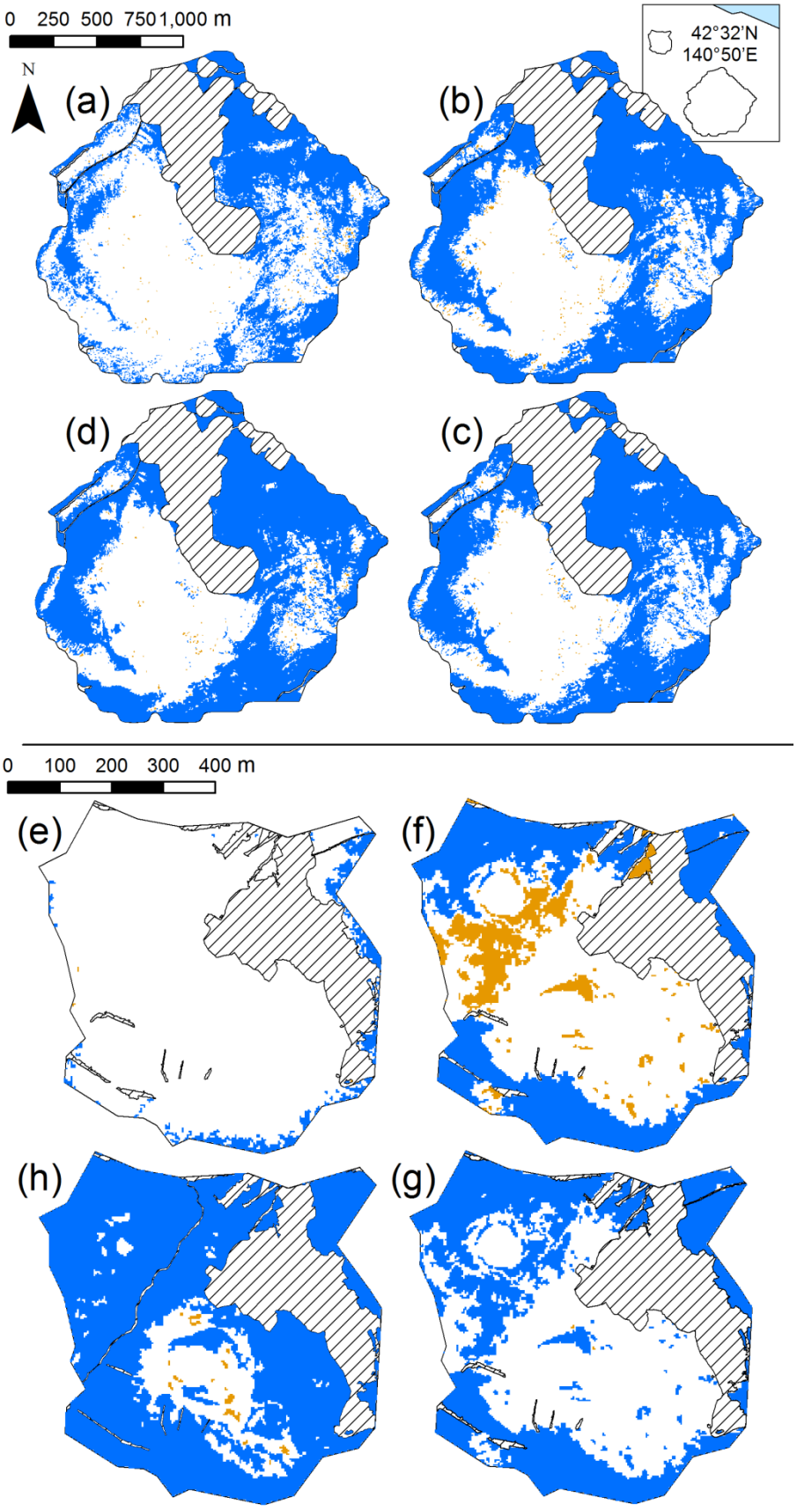
0 250 500 750 1,000 m
N
(a)
(b)
42°32'N
140°50'E
(d)
(c)
0 100 200 300 400 m
(e)
(f)
(h)
(g)

Figure 2. Vegetation patch establishment at the summit (a-d) and Konpira (e-h). The inset map shows the location of the summit (large area) and Konpira (small area) to each other. Alphabetical letters (a, b) and (e, f) mark 2000 and 2006, and show patch growth in the first period. Letters (c, d) and (g, h) mark 2006 and 2014 (from right to left), and show patch growth during the second period. Orange colour shows isolated patches and blue colour shows touching patches. The hatched areas are artificially influenced and excluded from the analysis, while white colour marks bare ground. Note that the scales are different between the summit and Konpira.

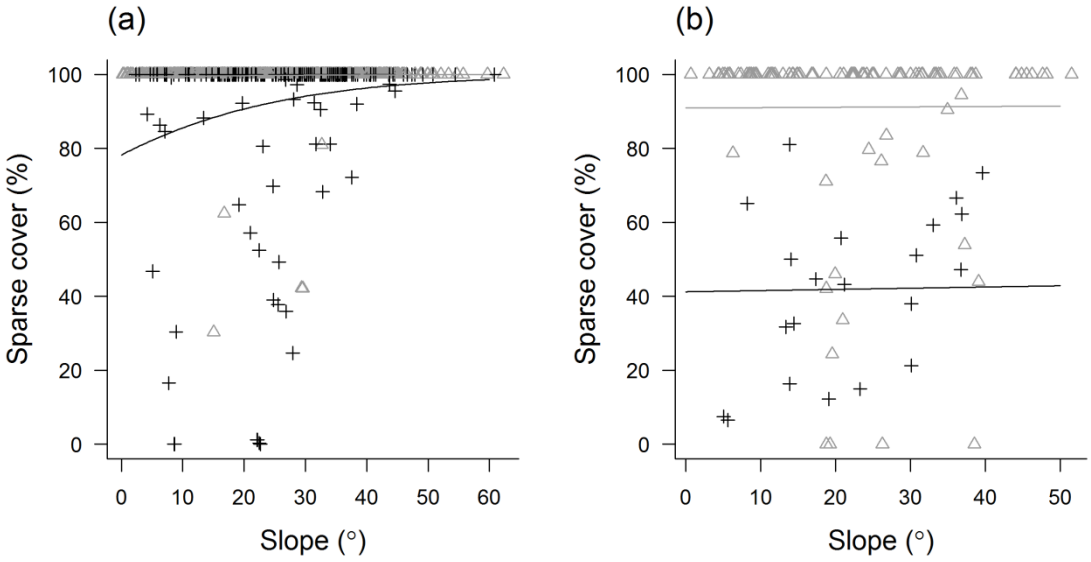

Figure 3. Effects of slope degree on vegetation density at the summit (a) and Konpira (b). Touching patches are marked by cross (+), while isolated patches are marked by (Δ). The response curves are generated by binomial GLM.

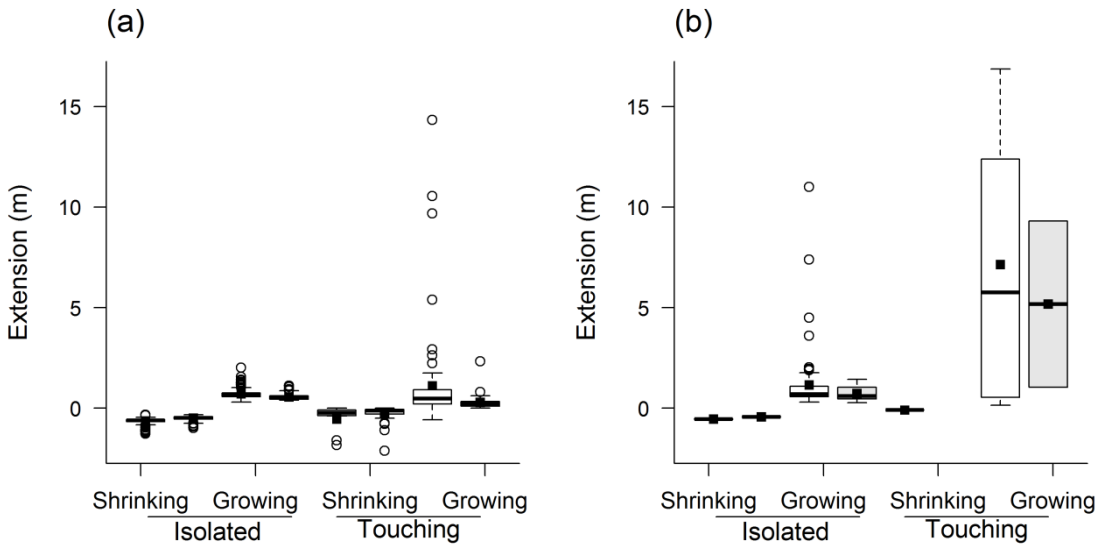

Figure 4. Annual growth (and shrinkage) of vegetation patches in relation to patch types and observation period at the summit (a) and at Konpira (b). Empty boxes mark the first period (2000–2006) and grey boxes mark the second period (2006–2014). The boxplots follow standard notation and the filled squares mark the means.

TABLE 1. Characteristics of the two eruption sites. The ranges of elevation and slope degree are shown with means in parentheses. Artificial areas were excluded from the study area for given year.

Study site		Summit	Konpira
Eruption year		1977–78	2000
Study area (ha)		291.43	37.91
Altitude (m)		400-732 (528)	111-271 (188)
Slope (°)		0-85 (25)	0-88 (26)
Artificial areas (ha)	2000	47.56	7.19
	2006	48.07	7.19
	2014	48.01	7.30

TABLE 2. Pearson's correlation coefficients between the Normalized Difference Vegetation Index values and Normalized Green-Red Difference Index values of satellite images. $P < 0.001$ in all cases.

Study area\Year	2006 (QuickBird)	2014 (Ikonos)
Summit	0.85	0.97
Konpira	0.39[a]	0.72[b]

[a]The low value is due to construction work in 2006. Human artefacts and open water surfaces are evaluated differently by the indices. After the exclusion of open water surfaces, the coefficient becomes 0.60.
[b]The low value is due to open water surfaces. After the exclusion of open water surfaces, the coefficient becomes 0.90.

TABLE 3. The accuracy of vegetation cover classification examined by Kappa coefficients. Confusion matrices show the relationships between the results obtained by index-based classification and visual validation. In every image acquisition year 300 randomly-selected points (100 points for Konpira and 200 for the summit) are used. NGRDI and NDVI are abbreviations of Normalized Green-Red Difference Index and Normalized Difference Vegetation Index.

2000 (Aerial)	Index based (NGRDI)		
Visual validation	No vegetation	Sparse vegetation	Dense vegetation
No vegetation	228	2	0
Sparse vegetation	0	22	2
Dense vegetation	0	2	44

Kappa = 0.95

2006 (Quickbird)	Index based (NDVI)		
Visual validation	No vegetation	Sparse vegetation	Dense vegetation
No vegetation	160	1	0
Sparse vegetation	0	72	0
Dense vegetation	0	2	65

Kappa = 0.98

2014 (Ikonos)	Index based (NDVI)		
Visual validation	No vegetation	Sparse vegetation	Dense vegetation
No vegetation	114	0	0
Sparse vegetation	0	84	0
Dense vegetation	0	2	100

Kappa = 0.99

TABLE 4. Patch characteristics compared between the patch types and eruption sites. The examined characteristics are: patches number, patch size, slope degree of patches, elevation and sparse cover percentage. Patch number is shown for all patch type, and mean of isolated or touching patches is shown with standard error in brackets. Mean values are compared by Wilcoxon rank sum test. Different letters on the upper-right of mean values indicate significant differences ($P < 0.001$ unless marked by *, where $P < 0.05$).

		Summit				Konpira			
Location		Isolated		Touching		Isolated		Touching	
Development		Growing	Shrinking	Growing	Shrinking	Growing	Shrinking	Growing	Shrinking
Patch	Period 1 (2000–2006)	303	169	75	19	79	3	8	1
number	Period 2 (2006–2014)	144	152	51	45	17	3	11	1
Slope (°)		25.5[a]	(0.4)	26.5[a]	(0.8)	22.9[a]	(1.2)	22.1[a]	(2.4)
Elevation (m)		542.4[b]	(3.1)	569.5[a]	(5.9)	187.9[c]	(3.9)	197.6[c]	(12.1)
Patch size (m^2)		57.5[c]	(1.3)	12,855.5[a]	(6,497.9)	337.6[b]*	(148.0)	12,258.2[a]	(8,179.7)
Patch sparse cover (%)		99.7[a]	(0.1)	92.1[b]	(1.6)	91.1[b]	(2.3)	41.9[c]	(4.9)

TABLE 5. Factors influencing the annual growth of vegetation patches. Only the significant effects are shown in the table (GLM, Gamma distribution with log link, ***: P < 0.001, **: P < 0.01).

Summit	Estimate	Std. Error	t value	
(Intercept)	-0.38	0.04	-10.24	***
Second period	-0.25	0.06	-4.19	***
Patch type – Touching	0.39	0.09	4.17	***
Interaction	-1.08	0.14	-7.96	***
Null deviance: 472.55 on 949 degrees of freedom				
Residual deviance: 385.61 on 946 degrees of freedom				

Konpira	Estimate	Std. Error	t value	
(Intercept)	1.69	0.45	3.76	***
Patch type – Touching	1.14	0.41	2.77	**
Sparse %	-0.02	0.00	-3.90	***
Null deviance: 107.804 on 102 degrees of freedom				
Residual deviance: 63.55 on 100 degrees of freedom				